Acta Crystallographica Section F
Structural Biology and Crystallization Communications
ISSN 1744-3091

Crystallization and preliminary X-ray crystallographic studies of human voltage-dependent anion channel isoform I (HVDAC1)

Thomas Meins,[a] Clemens Vonrhein[b] and Kornelius Zeth[c]*

[a]Max Planck Institute of Biochemistry, Department of Membrane Biochemistry, Am Klopferspitz 18, D-82152 Martinsried, Germany, [b]Global Phasing, Sheraton House, Castle Park, Cambridge CB3 0AX, England, and [c]Max Planck Institute of Developmental Biology, Department of Protein Evolution, Spemannstrasse 35, D-72076 Tübingen, Germany

Correspondence e-mail: kornelius.zeth@tuebingen.mpg.de

Received 3 April 2008
Accepted 2 June 2008

The major channel by which metabolites can pass through the outer mitochondrial membrane is formed by the voltage-dependent anion-channel (VDAC) family. Functionally, VDAC is involved in the limited exchange of ATP, ADP and small hydrophilic molecules across the outer membrane. Moreover, there is compelling evidence that VDAC isoforms in mammals may act in the cross-talk between mitochondria and the cytoplasm by direct interaction with enzymes involved in energy metabolism and proteins involved in mitochondrial-induced apoptosis. To obtain a high-resolution structure of this channel, human VDAC protein isoform I was overproduced in *Escherichia coli*. After refolding and testing the correct fold using circular dichroism, a subsequent broad-range screening in different detergents resulted in a variety of crystals which diffracted to 3.5 Å resolution. The crystal lattice belongs to the trigonal space group $P321$, with unit-cell parameters a = 78.9, c = 165.7 Å and one monomer in the asymmetric unit.

1. Introduction

The major connection *via* which metabolites overcome the outer mitochondrial membrane is formed by an aqueous pore known as eukaryotic porin. Owing to their ion-selective behaviour in conductance measurements, the channels are also termed voltage-dependent anion channels (VDACs; Benz, 1994; Colombini, 1980). As demonstrated by their characteristic voltage-dependent pore conductance, VDACs are capable of undergoing a reversible change from an open anion-selective to a semi-open cation-selective and ATP-impermeable state (Colombini, 1980). In addition to controlled and limited exchange of ATP, ADP and other small hydrophilic molecules of up to 600 Da, there is a strong indication that VDACs in mammals also provide an interface for the exchange of information between mitochondria and the cytosol. Different channel isoforms (HVDAC1–HVDAC3 in humans) therefore appear to be the potential target and anchor point of processes involving energy metabolism and the mitochondrial evolution of apoptosis (Shoshan-Barmatz & Gincel, 2003).

In energy metabolism, VDAC serves as the mitochondrial binding site for cytoplasmic hexokinases and glycerol kinases and connects these enzymes at mitochondrial contact sites with the ATP pool of the matrix space. As a consequence, a 'super' channel must be formed by adenine nucleotide translocator (ANT) and VDAC which allows preferential access to ATP through structural coupling of sites responsible for oxidative phosphorylation and metabolic activation. Dysfunction of the permeability transition pore formed by VDAC and ANT may lead to membrane rupture of the outer and inner membranes and the release of mitochondrial factors into the cytosol. Furthermore, VDAC is functionally regulated by the formation of transient complexes with cBid and Bcl-x_L, both of which belong to the Bcl-2 protein family (Green & Kroemer, 2004). These processes are likely to result in outer mitochondrial membrane permeabilization and hence mitochondrial dysfunction and apoptosis by release of cytochrome *c*.

Structurally, the 30 kDa VDAC protein is predicted to adopt a β-barrel fold similar to those of outer membrane proteins from Gram-negative bacteria. Evidence for a β-barrel structure for all

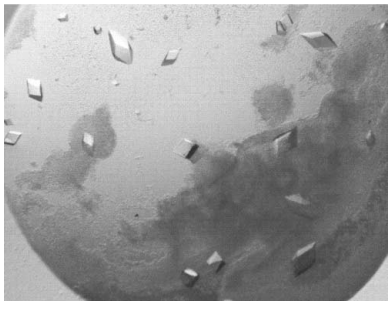

VDAC proteins studied to date has been derived from the incidence of amphipathic sequence patterns (Forte *et al.*, 1987) as well as from Fourier-transform infrared (Abrecht *et al.*, 2000) and circular-dichroism spectroscopy (Shao *et al.*, 1996). A channel structure similar in size and shape to that in bacterial analogues was further verified by electron micrographs of two-dimensional VDAC crystals from *Saccharomyces cerevisiae* (Guo & Mannella, 1993; Dolder *et al.*, 1999). Considering the ∼3.7 nm pore diameter deduced from electron microscopy, the secondary-structure contents and β-barrel geometries of a number of potential VDAC structures have been proposed. One model favours a small number (12–13) of β-strands, with the N-terminal helix being a transmembrane part of the channel wall (Blachlydyson *et al.*, 1990). In contrast, recent new models expect a 16-stranded (Casadio *et al.*, 2002; Engelhardt *et al.*, 2007) to 18-stranded (Mannella, 1997) barrel with an intra-luminally or extra-luminally located N-terminal helix.

Although VDAC is typically available in reasonable amounts in many cell types either by direct isolation from outer mitochondrial membranes or by overexpression in *Escherichia coli* and subsequent refolding (Koppel *et al.*, 1998; Shi *et al.*, 2003; Engelhardt *et al.*, 2007), structural studies have been hampered by the lack of three-dimensional crystals of this channel type. In this study, we present the first crystals suitable for X-ray structure determination of the human VDAC isoform I (HVDAC1) after insoluble overproduction in a bacterial expression system and successful refolding. The crystals obtained diffracted to a resolution of 3.6 Å.

2. Materials and methods

2.1. Cloning, expression, refolding and purification

A tagged version of HVDAC1 places four additional residues (MRGS–) at the N-terminus and eight consecutive residues (–RSHHHHHH) residues at the C-terminus. This His_6-tagged version of *hVDAC1* was achieved by cloning a *vdac1*-containing PCR construct into the PDS56/RBSII-6×His expression vector, yielding RBSII/VDAC1-His_6, as described elsewhere (Engelhardt *et al.*, 2007). For native HVDAC1-His_6 production, RBSII/VDAC1-6×His transformed *E. coli* ΔM15 (prep4) cells were grown in Terrific Broth medium at 310 K containing 100 mg l^{-1} ampicillin and 25 mg l^{-1} kanamycin. Adding 1 m*M* IPTG at an OD_{600} of 0.9 induced HVDAC1-His_6 inclusion-body formation. Cells were typically harvested after 4 h by centrifugation, resuspended in buffer 1 (100 m*M* Tris–HCl pH 7.5, 1 m*M* EDTA, 5 m*M* DTT, 100 m*M* NaCl, 0.2 m*M* PMSF) and incubated with 0.1 mg ml^{-1} lysozyme for 0.5 h. After addition of 1 m*M* $MgCl_2$, 0.1 m*M* $MnCl_2$ and 0.05 mg ml^{-1} DNAse I, cell lysis was carried out by two French press steps. Inclusion bodies were harvested by centrifugation at 5000*g* for 30 min at 277 K. The pellet was resuspended in buffer 1 containing 3%(*w*/*v*) *n*-octylpolyoxyethylene (OPOE), stirred for 2 h at room temperature and pelleted at 5000*g* for 30 min at 277 K. Finally, the pellet was washed with buffer 1 to remove detergent contamination. Inclusion bodies were then solubilized in buffer 2 (100 m*M* Tris–HCl pH 7.5, 1 m*M* EDTA, 5 m*M* DTT, 6 *M* guanidinium chloride) and insoluble material was removed by centrifugation at 100 000*g* for 45 min. The denatured HVDAC1-His_6 protein-containing supernatant was stored at 203 K until use.

HVDAC1-His_6 refolding was performed at 277 K by dropwise dilution of solubilized protein in buffer 3 [100 m*M* Tris–HCl pH 8.0, 1 m*M* EDTA, 5 m*M* DTT, 1%(*w*/*v*) LDAO] until a final concentration of 0.6 *M* guanidinium chloride was reached. The resulting protein solution was stirred overnight at 277 K, centrifuged at 100 000*g* for 45 min and finally diluted fivefold with buffer 4 (100 m*M* phosphate buffer pH 7.5). HVDAC1-His_6 was then bound to a 5 ml Ni^{2+}-Sepharose HP column (GE Healthcare), washed with 100 ml buffer 5 (20 m*M* phosphate buffer pH 7.5, 20 m*M* imidazole, 0.6% OPOE) and then eluted with 50 ml buffer 6 (20 m*M* phosphate buffer pH 7.5, 300 m*M* imidazole, 0.6% OPOE).

Fractions containing HVDAC1-His6 were analyzed by SDS–PAGE, pooled and concentrated with a centrifugal filter device (Amicon Ultra-30K, Millipore) to concentrations between 5 and 15 mg ml^{-1}. Samples were finally extensively dialysed against 0.067% Cymal-5 in buffer 7 (20 m*M* bis-Tris–HCl pH 6.8; Table 1) for 60 h to completely remove OPOE and stored at 277 K until use. The absence of any other detergent used previously was shown by electrospray mass spectrometry.

Table 1
Summary of the crystallization trials using various detergents.

Conc. indicates the initial concentration of detergent in the crystallization drop. The numbers in parentheses give the number of different crystallization condition in which crystals appear out of the 334 used. C_8E_4, *n*-octyltetraoxyethylene; $C_{10}E_8$, *n*-octaethylene glycol monodecylether; $C_{12}E_9$, nonaethylene glycol monododecylether; OPOE, *n*-octylpolyoxyethylene; OG, *n*-octyl-β-D-glucopyranoside; NG, *n*-nonyl-β-D-glucopyranoside; NM, *n*-nonyl-β-D-maltopyranoside; DM, *n*-decyl-β-D-maltopyranoside; UM, *n*-undecyl-β-D-maltopyranoside; DDM, *n*-dodecyl-β-D-maltopyranoside; DDAO, *N*,*N*-dimethyldecylamine-β-oxide; LDAO, lauryldimethylamine oxide; Cymal-3, cyclohexylpropyl-β-D-maltoside; Cymal-4, cyclohexylbutyl-β-D-maltoside; Cymal-5, cyclohexylpentyl-β-D-maltoside; Cymal-6, cyclohexylhexyl-β-D-maltoside

Detergent	Conc. (%)	Crystals (conditions)	Resolution (Å)
C_8E_4	0.67	+ (2)	>30
$C_{10}E_8$	0.067	–	
$C_{12}E_9$	0.067	+ (2)	>30
OPOE	0.33	+ (5)	>8
OG	0.5	–	
NG	0.17	–	
NM	0.23	–	
DM	0.1	+ (8)	>20
UM	0.067	–	
DDM	0.33	+ (9)	>30
DDAO	0.17	+ (27)	>8
LDAO	0.067	+ (22)	>15
Cymal-3	0.67	–	
Cymal-4	0.2	–	
Cymal-5	0.067	+ (9)	3.5
Cymal-6	0.20	–	

2.2. Secondary-structure determination by circular-dichroismn spectroscopy

CD spectra from HVDAC1-His_6 samples (0.25 mg ml^{-1} protein in 10 m*M* Tris–HCl pH 8 supplemented with 0.2% LDAO) were recorded on a Jasco J-810 spectrophotometer in a 0.1 mm quartz cuvette at 277 K. Ten spectra were accumulated per measurement, using a data pitch of 0.1 nm, a scan speed of 20 nm s^{-1}, a 1 nm slit width and a response time of 2 s. Spectral analysis was performed with the deconvolution software *CDNN* v.2.1.

2.3. Crystallization and X-ray crystallographic analysis

Crystallization trials were performed using screens from Hampton Research. Crystallization was induced by the hanging-drop vapour-diffusion method. 1.5 µl HVDAC1-His_6 samples were mixed with 0.75 µl precipitant solution and equilibrated against 0.5 ml precipitant solution at 291 K.

For the initial crystallization setup, we used protein samples in various detergents. Crystallization was achieved in many, but not all, protein–detergent micelles. Our best results were obtained with Cymal-5 under crystallization conditions containing 30% PEG 400, 0.1 *M* Na HEPES pH 7.5, 0.2 *M* magnesium chloride. Crystals were

Table 2
Data-collection statistics.

Values in parentheses are for the highest resolution shell.

Beamline	PX10, SLS
Detector	MAR CCD 225 mm
Crystal-to-detector distance (mm)	400
Wavelength (Å)	0.954
Crystal	TM10
Space group	*P*3221
Systematic absences	(0, 0, 3*n*)
Unit-cell parameters (Å, °)	a = 78.9, b = 78.9, c = 165.7, α = 90, β = 90, γ = 120
Resolution (Å)	40.00–3.6 (3.81–3.50)
Mosaicity	1.07
Measured reflections	51117 (8029)
Unique reflections	7223 (1105)
Redundancy	7.1 (7.3)
Completeness (%)	98.3 (99.9)
R_{merge}† (%)	10.8 (66.1)
Mean $I/\sigma(I)$	11.08 (3.02)

† $R_{merge} = \sum_{hkl} \sum_i |I_i(hkl) - \langle I(hkl)\rangle| / \sum_{hkl} \sum_i I_i(hkl)$.

harvested and frozen directly in liquid nitrogen. In order to prove that the protein forming the crystal was HVDAC1, crystals from the same condition were collected manually, washed in the corresponding reservoir solution and redissolved in water; the protein was then verified by (i) N-terminal peptide sequencing and (ii) SDS–PAGE. Native data collection was performed on beamline PX10 of the SLS (Swiss Light Source, Villigen, Switzerland) synchrotron-radiation source. Measurements were carried out at 100 K under the experimental setup described in Table 2. All data were indexed, integrated and scaled with *XDS* (Kabsch, 1993).

3. Results and discussion

In the human genome, three isoforms of the voltage-dependent anion-channel are known (*hvdac1–3*). However, the most abundant protein in the mitochondrial outer membrane of mammals is also the currently best described form in the literature and is termed isoform I or HVDAC1 protein (Gonçalves *et al.*, 2007). This isoform was therefore used as a basis for further structural analysis. It has previously been shown that HVDAC1 protein was able to form highly ordered protein arrays in two dimensions that were appropriate for electron microscopy (Dolder *et al.*, 1999).

In order to obtain diffracting crystals suitable for structure determination of VDAC, we started with a vector encoding the human mitochondrial isoform I. We expressed the human protein with a C-terminal His tag in *E. coli*. This approach resulted in inclusion-body formation of multimilligram quantities of HVDAC1, in analogy to previous studies of related proteins (Koppel *et al.*, 1998; Shi *et al.*, 2003; Engelhardt *et al.*, 2007). After solubilization, purification and refolding, the recovery of HVDAC1 from 1 l of cell culture yielded approximately 50 mg.

Successful refolding of the protein was confirmed by far-UV CD spectroscopy in 0.2% LDAO at pH 7 (Fig. 1). The spectra recorded, which have an intercept in ellipticity ($\lambda_{crossover}$) of 204 nm and a broad minimum of ellipticity (λ_{min}) around 215 nm, resemble the data for mitochondrial VDAC proteins from other organisms (Shao *et al.*, 1996). Spectral deconvolution of the recorded spectrum predicted a fold with ∼12% α-helical, ∼26% β-sheet and ∼15% β-turn structure, which is in agreement with previous data for the same VDAC analyzed by FTIR (Engelhardt *et al.*, 2007) and for scVDAC from *Saccharomyces cerevisiae* (35% β-sheet, 20% α-helix, 17% β-turn) which was critically dependent on pH values and the detergent used (Koppel *et al.*, 1998).

The large amount of HVDAC1 obtained by the method described facilitated the use of a variety of detergents for crystallization. The refolding process was induced in the presence of LDAO, while exchange against OPOE was achieved during column chromatography. On screening different detergents, pH values, precipitating agents and buffers against 5400 different crystallization conditions, HVDAC1 produced crystals under 84 different conditions (Table 1). Crystals typically appeared after 7–14 d over a broad range of detergent classes. For the crystallographic data shown here, crystals obtained using Cymal-5 were used. These crystals exhibited a rhombohedric morphology (Figs. 2*a* and 2*b*). Although most of the crystals obtained appeared similar in shape and size, only a very few were suitable for data collection. A resolution of 3.6 Å was achieved from Cymal-5-solubilised protein (Figs. 2*a*, 2*b* and 3). The content of these crystals could be verified by SDS–PAGE and N-terminal sequencing of dissolved crystals (Fig. 1*c*). Analysis of the diffraction data revealed the crystal form to be one of the trigonal space groups, with systematic absences (0, 0, 3*n*). The unit-cell parameters are a = 78.9, c = 165.7 Å. $\alpha = \beta = 90$, $\gamma = 120°$. Scaling of the collected data indicated an R_{merge} of 10.8%, a mean $I/\sigma(I)$ of 11.08 and a solvent content of 65% assuming the presence of one monomer and an unknown number of detergent molecules in the asymmetric unit. While the R_{merge} value for the outer shell is rather high, we are proceeding for now at 3.6 Å resolution and will not reduce the resolution until the experiments show that reduction is needed.

The structure of the protein will be pursued using two different approaches: (i) introduction of additional methionines into the wild-type protein sequence to improve the anomalous signal during data collection for MAD/SAD and (ii) analysis of NMR data of the protein to produce a NMR model to use in combination with experimental and model phases in phasing programs.

The results presented here support the successful crystallization of a mitochondrial porin. The structures of proteins from the outer

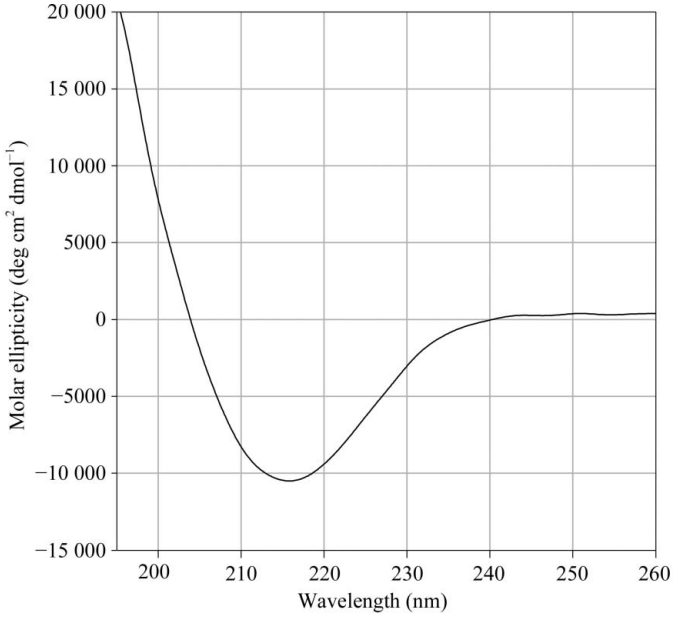

Figure 1
CD spectrum of HVDAC1-His$_6$ after refolding in C_8E_4. The intercept in ellipticity ($\lambda_{crossover}$) of 204 nm and the ellipticity minimum (λ_{min}) at 215 nm correspond almost ideally to the values for other mitochondrial VDAC proteins (Shao *et al.*, 1996).

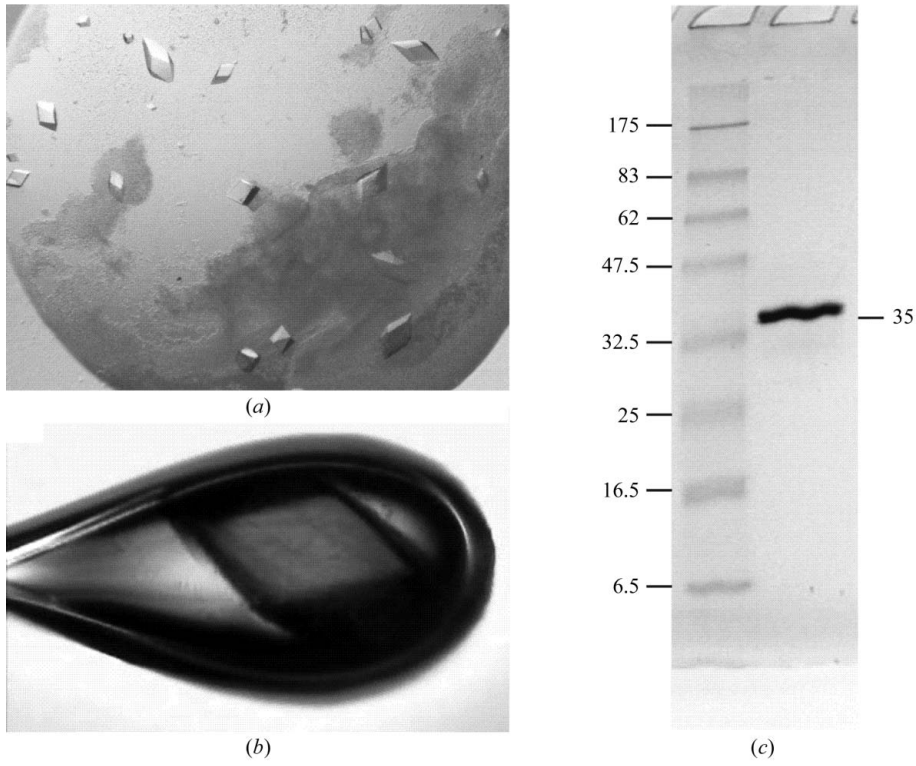

Figure 2
Pictures of the rhombohedral HVDAC1-His_6 crystals with dimensions of 0.2 × 0.1 × 0.1 mm in the crystallization drop (*a*) and in a loop (*b*). (*c*) Representation of a Coomassie-stained 15% SDS–PAGE gel loaded with dissolved crystals shown in (*a*) and (*b*). Molecular weights are labelled in kDa.

membrane of mitochondria are not known and the structure of VDAC may form the first example of this class of proteins. Insights gained from a VDAC structure will be valuable with respect to structure comparisons of the bacterial homologues. Moreover, HVDACs have been described as potential targets for pharmaceutical research and a structure of this human protein at higher resolution may provide an ideal basis for modelling studies. Complex structures with proteins involved in VDAC regulation, *i.e.* tBid, are planned in order to study the structural differences known to occur upon complex formation.

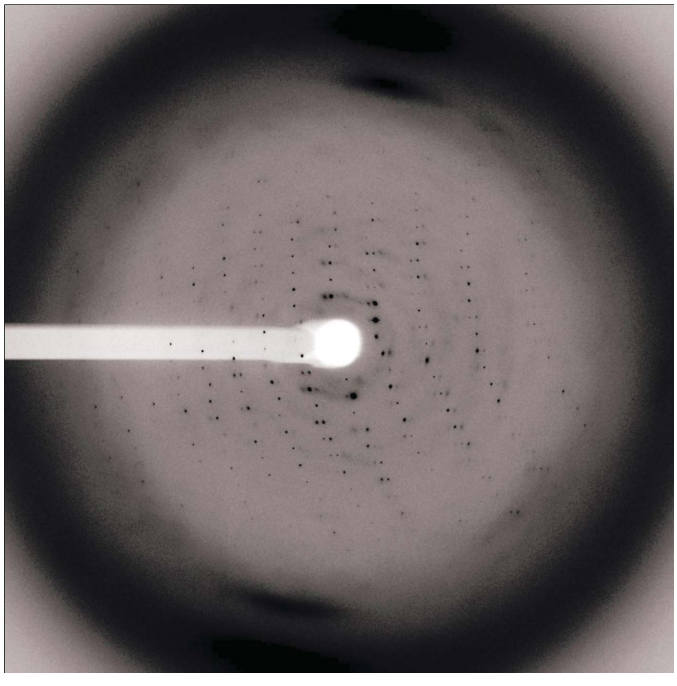

Figure 3
Diffraction pattern of the HVDAC1-His_6 crystal shown in Fig. 2 recorded on beamline PX10 at SLS.

The authors cordially thank Dr Ehmke Pohl from beamline PX10 for his excellent technical assistance and beamline support. We would also like to thank the staff of the SLS, Villigen for maintenance and operation of the protein crystallography beamlines. Furthermore, we thank Elisabeth Weyher-Stingl for recording and analysis of the CD data and Reinhard Mentele for N-terminal sequencing. The authors also thank Professor Dieter Oesterhelt, Max Planck Institute of Biochemistry for continuous interest and support.

References

Abrecht, H., Goormaghtigh, E., Ruysschaert, J. M. & Homble, F. (2000). *J. Biol. Chem.* **275**, 40992–40999.
Benz, R. (1994). *Biochim. Biophys. Acta*, **1197**, 167–196.
Blachlydyson, E., Peng, S. Z., Colombini, M. & Forte, M. (1990). *Science*, **247**, 1233–1236.
Casadio, R., Jacoboni, I., Messina, A. & De Pinto, V. (2002). *FEBS Lett.* **520**, 1–7.
Colombini, M. (1980). *Ann. NY Acad. Sci.* **341**, 552–563.
Dolder, M., Zeth, K., Tittmann, P., Gross, H., Welte, W. & Wallimann, T. (1999). *J. Struct. Biol.* **127**, 64–71.
Engelhardt, H., Meins, T., Poynor, M., Adams, V., Nussberger, S., Welte, W. & Zeth, K. (2007). *J. Membr. Biol.* **216**, 93–105.
Forte, M., Guy, H. R. & Mannella, C. A. (1987). *J. Bioenerg. Biomembr.* **19**, 341–350.
Gonçalves, R. P., Buzhynskyy, N., Prima, V., Sturgis, J. N. & Scheuring, S. (2007). *J. Mol. Biol.* **369**, 413–418.
Green, D. R. & Kroemer, G. (2004). *Science*, **305**, 626–629.
Guo, X. W. & Mannella, C. A. (1993). *Biophys. J.* **64**, 545–549.

Kabsch, W. (1993). *J. Appl. Cryst.* **26**, 795–800.
Koppel, D. A., Kinnally, K. W., Masters, P., Forte, M., Blachly Dyson, E. & Mannella, C. A. (1998). *J. Biol. Chem.* **273**, 13794–13800.
Mannella, C. A. (1997). *J. Bioenerg. Biomembr.* **29**, 525–531.
Shao, L., Kinnally, K. W. & Mannella, C. A. (1996). *Biophys. J.* **71**, 778–786.
Shi, Y., Jiang, C., Chen, Q. & Tang, H. (2003). *Biochem. Biophys. Res. Commun.* **303**, 475–482.
Shoshan-Barmatz, V. & Gincel, D. (2003). *Cell Biochem. Biophys.* **39**, 279–292.